

Optimal Enhancement of Brain Structures by Combining Different MR Contrasts: Demonstration of Venous Vessel Enhancement in Multi-Echo Gradient-Echo MRI

Andreas Deistung¹, Ferdinand Schweser¹, and Jürgen Rainer Reichenbach¹

¹Medical Physics Group, Institute of Diagnostic and Interventional Radiology I, Jena University Hospital - Friedrich Schiller University, Jena, Germany

TARGET AUDIENCE: Researchers with interest in venous vessel visualization, susceptibility weighted imaging, and novel MR image contrasts.

PURPOSE: Multi-echo gradient-recalled echo (GRE) sequences provide quantitative information about the effective transverse relaxation rate, R_2^* , (magnitude of the signal) and magnetic field perturbations caused by the tissue susceptibility distribution (phase of the signal). They also reveal information of the magnitude signal immediately after the rf-pulse, S_0 , which depends on tissues' spin density and T_1 as well as on the flip angle.¹ The complex GRE information is, for instance, employed in susceptibility weighted imaging (SWI), a heuristic approach for combining magnitude and phase of the GRE signal into a composite image to enhance the contrast of cerebral veins and brain lesions.^{2,3} While SWI is today established in hospitals throughout the world a considerable drawback of SWI is that the visualization of veins depends on the orientation of the vessels with respect to the main magnetic field. This is reflected in sometimes ambiguous representations of veins, in particular in sagittal and coronal views, and impedes accurate segmentation of cerebral veins and quantification of their radii. Automatic generation of 3D models of the venous vasculature based on SWI is also hampered because the inter-hemispheric fissure is hypointensely displayed, just like veins. In this contribution, we present a supervised approach for creating image contrast that enhances specific structures of interest. We apply linear discriminant analysis (LDA) to optimally combine multiple image contrasts generated from complex-valued multi-echo GRE information (magnetic susceptibility, R_2^* , and S_0) to yield a novel contrast with increased venous vessel contrast.

THEORY: LDA⁴ is a technique for feature extraction and dimension reduction. LDA projects data onto a lower-dimensional vector space such that the ratio of the between-class distance to the within-class distance is maximized, thus achieving maximum discrimination. Volumes of interest (VOIs) were identified in 4 subjects and the means and standard deviations of magnetic susceptibility, R_2^* , and S_0 were assigned as features. VOIs were divided into two classes: vein (central and cortical veins, sinus rectus) and remaining tissue (arteries, cerebrospinal fluid (CSF), white matter (WM), cortical gray matter (GM), deep GM structures, interhemispheric fissure). LDA was applied to these data (training step) and the resulting base vectors were then applied to other GRE data (evaluation step) to generate composite images.

METHODS: Dual-echo GRE data sets (TOF-SWI-sequence,⁵ $TE_1/TE_2/TR/FA/TA=3.5\text{ ms}/25.4\text{ms}/15^\circ/13:31\text{min:sec}$, voxel size = $0.45\text{mm} \times 0.45\text{mm} \times 1.2\text{mm}$) were acquired from six healthy volunteers on a 3T MR scanner. Four data sets were employed to find the optimal base vectors using LDA (training step) which were then evaluated on the remaining two data sets (evaluation step). Maps of R_2^* (in ms^{-1}) and S_0 were computed using mono-exponential fitting of the magnitude signal decay. Aliasing in phase images was resolved by 3D phase unwrapping⁶ and background phase contributions were eliminated with the SHARP method.⁷ Homogeneity enabled incremental dipole inversion⁸ of the background-corrected phase images yielded quantitative susceptibility maps. To reduce inter-subject variability, the magnetic susceptibility was normalized with respect to frontal white matter ($\Delta\chi$), and the range of S_0 values was adjusted to be between 0 and 1. For comparison, SW images were created from magnitude and phase images according to the SWI standard processing scheme (i.e., 4-fold multiplication of the linearly weighted high-pass filtered phase images with the magnitude images).^{2,3} Venous vessel visibility was assessed by computing the contrast-to-noise ratio (CNR) of 5 veins for the different contrasts according to $\text{CNR} = |(S_v - S_t)/\sigma_t|$, where S and σ denote the mean and standard deviation of a VOI and the subscripts v and t indicate whether the VOI represents a vein or tissue.

RESULTS: Mean R_2^* values were plotted against mean magnetic susceptibility differences (Fig. 1). Although the majority of veins were characterized by high susceptibilities, certain deep GM structures (globus pallidus, substantia nigra, and red nucleus; black points in Fig. 1) yielded similar susceptibility and R_2^* values, resulting in a slight overlap between the two classes. LDA yielded maximum separation if $\Delta\chi$ and R_2^* were merged according to: $0.447\text{ ppm}^{-1} \cdot \Delta\chi + 0.894\text{ s} \cdot R_2^* - 0.049$ and if $\Delta\chi$, R_2^* , and S_0 were combined according to $0.325\text{ ppm}^{-1} \cdot \Delta\chi + 0.907\text{ s} \cdot R_2^* - 0.27 \cdot S_0 - 0.013$. The LDA-combined images are presented in Fig. 2e and f. In these images the apparent intensity of CSF increased (blue arrow in Fig. 2) and of highly myelinated regions decreased (red arrow in Fig. 2) compared to the magnetic susceptibility map. Furthermore, the inter-hemispheric fissure was displayed isointense on LDA-combined images (black arrows in Fig. 2e and f). The sinus veins were accurately displayed in the composite image, whereas hypointensities around veins were observed in SW images (red arrows in Fig. 3). The average CNR was highest for the LDA-combined image based on $\Delta\chi$, R_2^* , and S_0 (CNR=6.46). The CNR of the remaining contrasts were: 4.70 for magnetic susceptibility, 4.46 for R_2^* , 4.31 for the magnitude, 5.12 for SWI, and 6.01 for the LDA-combined data based on $\Delta\chi$ and R_2^* .

DISCUSSION: Base vectors derived from discriminant analysis of training data allowed the combination of multiple contrasts into composite images that yielded increased venous contrast compared to the magnetic susceptibility and R_2^* maps alone. The base vectors can also be transferred to data collected with different acquisition parameters because magnetic susceptibility is nearly independent of acquisition parameters and the dependence of acquisition parameters on R_2^* can be considered. The venous contrast, in particular in deep GM regions, may be further improved by incorporating additional features obtained after post-processing of GRE data (e.g., application of vessel enhancing diffusion filtering¹⁰ to magnetic susceptibility images) or additional MRI scans as well as employing non-linear discriminant analysis.¹¹ The presented approach may be applied as a pre-processing step in order to segment veins from GRE data using image-based approaches, such as active contours, or the base vectors obtained by discriminant analysis may be interpreted as classifier.

CONCLUSION: Discriminant analysis provides base vectors for optimized combination of multiple contrasts. The technique can be easily adjusted to emphasize other tissue properties in composite images by changing the definition of classes in the training step to yield, e.g., improved delineation of pathologies such as cortical lesions.

REFERENCES: [1] Haacke EM et al. *Magnetic Resonance Imaging: - Physical Principles and Sequence Design*. 1999. John Wiley & Sons, Inc. [2] Reichenbach JR et al. *Radiology* 1997;204(1):271-7. [3] Haacke EM et al. *Magn Reson Med*. 2004;52(3):612-8. [4] McLachlan GJ. *Discriminant Analysis and Statistical Pattern Recognition*. 1992. John Wiley & Sons, Inc. [5] Deistung A et al. *J Magn Reson Imaging*. 2009;29(6):1478-84. [6] Abdul-Rahman HS et al. *Appl Opt*. 2007;46(26):6623-3. [7] Schweser F et al. *NeuroImage*. 2011;54(4):2789-807. [8] Schweser F et al. *NeuroImage*. 2012;62(3):2083-100. [10] Mannesingh R et al. *Med Image Anal*. 2006;10(6):815-825. [11] Baudat G and Anouar F. *Neural Computation*, 12(10):2385-2404, 2000.

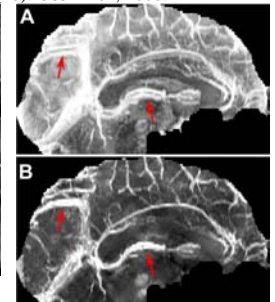
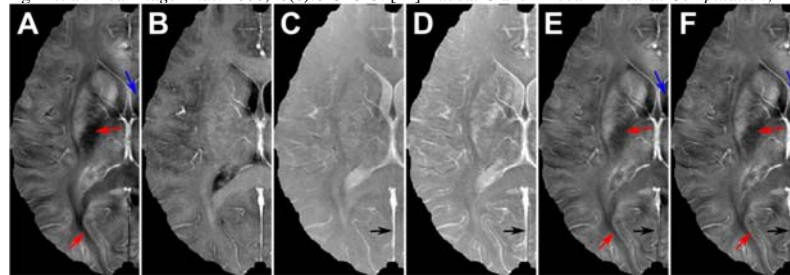
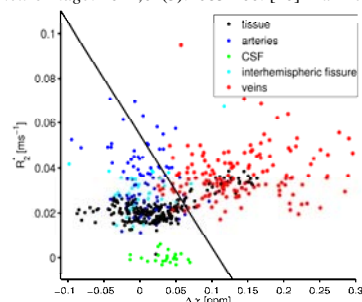


Figure 1: R_2^* plotted against magnetic susceptibility differences ($\Delta\chi$) with respect to frontal WM. The principle axis obtained by LDA (black line) provides the best separation between the two groups (veins vs. remaining tissue [tissue, arteries, CSF, inter-hemispheric fissure]).

Figure 2: Transverse average intensity projections over 6 mm of magnetic susceptibility maps (a), R_2^* maps (b), magnitude (c; $TE=25.4\text{ms}$), SWI (d), composite image based on magnetic susceptibility, R_2^* and S_0 (e), and composite image based on magnetic susceptibility, R_2^* and S_0 (f), respectively. Blue and red arrows indicate CSF and regions with high myelin content, respectively. The black arrows point to the inter-hemispheric fissure that LDA-combination based on isointense on the composite images (e,f) and hyperintense on the inverted SWI (d). For magnetic susceptibility, R_2^* and S_0 are shown in (a) and (b).

Figure 3: Sagittal maximum intensity projection across 12 mm at the level of inter-hemispheric fissure of inverted SWI and the magnitude of comparison. The top row (A) shows the magnitude of comparison, and the bottom row (B) shows the inverted SWI. Red arrows indicate CSF and regions with high myelin content, and black arrows indicate the inter-hemispheric fissure.